

Grant Agreement No: 101094300

MuCoL

A Design Study for a Muon Collider complex at 10 TeV centre of mass
Horizon Europe Framework Programme

DELIVERABLE REPORT

DEVELOPMENT OF BDSIM SIMULATION

DELIVERABLE: D4.1

Document identifier:	MuCol_D4.1_final.pdf
DOI:	10.5281/zenodo.14943349
Due date of milestone:	28/02/2025 (End of Month 24)
Justification for delay:	N/A
Work package:	WP4: Muon Production & Cooling
Lead beneficiary:	Imperial
Report release date:	25/02/2025
Document version:	1.0
Document status:	Final

Abstract:

This report summarises the extension of the capabilities of the Beam Delivery Simulation (BDSIM) code to support ionization cooling simulations for muon collider studies. We have developed and integrated a new muon cooler beamline element within BDSIM. This implementation allows for the simulation of arbitrary configurations of high-field solenoids, RF cavities, dipoles, and absorbers, enabling comprehensive modelling of ionization cooling channels. The new functionality ensures that BDSIM is now a powerful and versatile tool for muon collider design studies, supporting detailed simulations of the full muon collider cooling system.

MuCol Consortium, 2025

For more information on MuCol, its partners and contributors please see <https://mucol.web.cern.ch/>

Funded by the European Union (EU). Views and opinions expressed are however those of the author(s) only and do not necessarily reflect those of the EU or European Research Executive Agency (REA). Neither the EU nor the REA can be held responsible for them.

Delivery Slip

	Name	Partner	Date
Authored by	P. Jurj, R. Kamath, J. Pasternak C. Rogers	Imperial UKRI	25/02/25
Edited by	C. Rogers	UKRI	25/02/25
Reviewed by	J. Pasternak [Task coordinator] C. Rogers [WP coordinator] R. Losito [Scientific coordinator]	Imperial UKRI CERN	25/02/25
Approved by	R. Losito [Scientific coordinator] MuCol Management Committee	CERN	25/02/25

Contents

1	Introduction	4
2	Physics Models	4
2.1	Dipole	5
2.2	Solenoid	6
2.2.1	Solenoid Sheet	7
2.2.2	Solenoid Block	8
2.2.3	Tolerances and bounding boxes	8
2.3	RF Cavities	9
3	Implementation	9
3.1	Source Code and Version Control	9
3.2	Components	9
3.3	Electric and Magnetic Field Models	10
3.4	Parameters	10
3.5	Visualisation	12
4	Validations	12
4.1	Dipole	12
4.2	Solenoid	16
4.3	RF Cavities	19
4.4	Absorbers	20
4.5	Full Lattice	22
4.5.1	4D Cooling	22
4.5.2	Rectilinear (6D) Cooling	22
5	Conclusion and Future Work	25

1 Introduction

The muon collider is an excellent prospect as a multi-TeV lepton collider, with the possibility for high luminosity and reach to 10 TeV centre-of-mass energy per parton. In order to realise high luminosity, high beam brightness is required. Ionisation cooling, which was demonstrated by the Muon Ionization Cooling Experiment (MICE) [1], is the technique proposed to realise sufficient brightness. The muon collider ionisation cooling system is composed of a series of solenoids, which tightly focus the beam onto energy absorbers where the beam momentum is removed. The momentum is restored longitudinally using radiofrequency (RF) cavities, resulting in a reduction of the volume in position-momentum space occupied by the beam. This volume is characterised by the normalised beam emittance. An initial rectilinear cooling system reduces the beam emittance sufficiently that the many initial bunches can be merged into one single bunch. The beam is then cooled further to the target emittance by a second rectilinear cooling system followed by a so-called final cooling system, a sequence of high-field solenoids operated ultimately with a low-momentum (non-relativistic) beam.

The rectilinear cooling and final cooling systems contain about 20 different arrangements of cooling cells, each with various geometry, length, magnetic field strength, RF electric field and frequency [2]. The design of these systems and their performance assessment is highly reliant on simulation studies. Currently, G4Beamline [3] is the main software employed by the MuCol study, with RFTrack [4] also being developed and used for final cooling studies. The use of multiple simulation tools is essential for cross-validation, ensuring the robustness of design choices and mitigating the limitations inherent to any single software package. Hence, there is scope for using additional codes, such as BDSIM, to further enhance the reliability of the cooling simulations.

The Beam Delivery Simulation software (BDSIM) [5], developed in Europe to model accelerator lattices in the presence of beam-intersecting devices, has been used for studies of next-generation collider candidate facilities such as FCC-hh, CLIC, and ILC. While previous and current ionisation cooling simulations relied on G4Beamline, this software has not been updated in several years, leading to a need for a more actively maintained and flexible alternative. BDSIM has emerged as a strong candidate for muon cooling simulations, offering a modern Geant4-based framework [6] with ongoing development and support. Initial work on developing the muon cooling capabilities in BDSIM, focused on implementing the framework for an ionisation cooling-dedicated beamline element, was done by L. Nevay [7]. The work presented here summarises the implementation and integration of all the physical models of the lattice components required for six-dimensional ionisation cooling, along with various model extensions and code optimisations.

The structure of the report is as follows. The underlying physics models of each of the components of a 6D cooling channel have been described in Sec. 2. The structure of their implementation and a description of their integration into BDSIM is outlined in Sec. 3. Validations and demonstrations to ensure the simulations are working as expected have been done and results have been included in Sec. 4. The conclusions and future prospects have been described in Sec. 5.

2 Physics Models

A rectilinear 6D cooling cell (Fig. 1) consists of four distinct types of components: solenoid coils, RF cavities, dipole magnets, and wedge-shaped energy absorbers. The dipoles, in conjunction with

the wedge absorbers, enable emittance exchange and hence 6D cooling, as follows: first the dipole generates a position-energy correlation, as higher energy particles have a large bending radius. Then a wedge absorber is arranged such that the higher energy particles traverse the thicker part of the absorber, losing more energy. This reduces the beam energy spread while the position spread is increased - the emittance is moved from longitudinal space to transverse space.

The models of the electromagnetic fields generated by the solenoids, RF cavities, and dipoles have been implemented in C++ language into the BDSIM source code. Models for particle-matter interactions are inherited from and handled by the underlying GEANT4 framework.

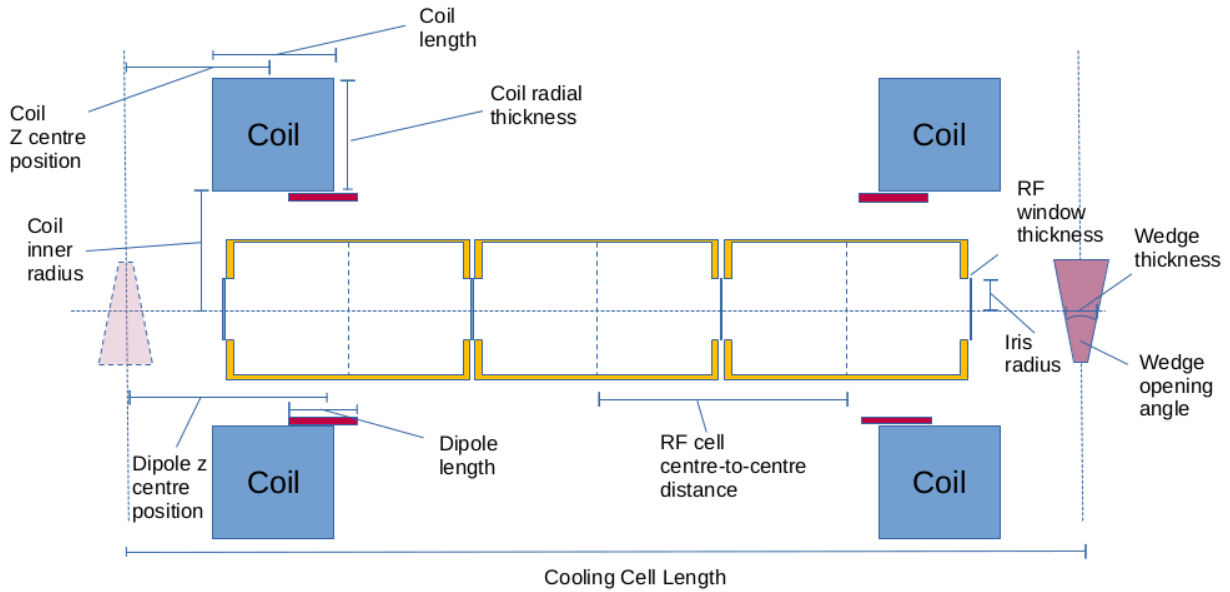


Figure 1: Schematic of the Muon Cooling Demonstrator cooling cell produced by WP8 [8].

2.1 Dipole

The dipole magnets used in the rectilinear cooling lattice have a large aperture relative to their on-axis length. Hence, the dipole field is fringe-field dominated – fringe fields are regions at the end of a magnet where the field transitions from a nominal value inside the magnet to zero field or to the field in a neighbouring magnet. To realistically model such a field, we implemented a dipole field model derived from the treatment described by Muratori et al. in [9], which models the fringes as Enge functions.

The fringe fields are of the form

$$B_y = B_0 \left(\frac{1}{2(1 + e^{E(z+iy)})} + \frac{1}{2(1 + e^{E(z-iy)})} \right) \quad (1)$$

$$B_z = B_0 \left(\frac{-i}{2(1 + e^{E(z+iy)})} + \frac{i}{2(1 + e^{E(z-iy)})} \right) \quad (2)$$

where B_0 is the peak dipole field in the body of the magnet and $E(Z)$ is a polynomial, given by

$$E(Z) = \sum_{n=0}^{N-1} a_n \left(\frac{Z}{D} \right)^n. \quad (3)$$

The function has an arbitrary number N of terms weighted by a_n coefficients and D is the aperture of the magnet. The number of terms in the summation can be adapted to customise the shape of the fringe field falloff. For simplicity, we set all coefficients a_n to 0 except for a_1 and $B_0 = 1$, and equations 1 and 2 reduce to

$$B_y = \frac{1 + e^{\alpha z} \cos \alpha y}{1 + 2e^{\alpha z} \cos \alpha y + e^{2\alpha z}}, \quad (4)$$

$$B_z = \frac{-e^{\alpha z} \sin \alpha y}{1 + 2e^{\alpha z} \cos \alpha y + e^{2\alpha z}}, \quad (5)$$

where $\alpha = a_1/D$.

A complete description of the dipole field requires including both the entry (left) and exit (right) fringe fields, given by

$$B_{y,l} = \frac{1 + e^{-\alpha z_l} \cos \alpha y}{1 + 2e^{-\alpha z_l} \cos \alpha y + e^{-2\alpha z_l}}, \quad (6)$$

$$B_{z,l} = \frac{e^{-\alpha z_l} \sin \alpha y}{1 + 2e^{-\alpha z_l} \cos \alpha y + e^{-2\alpha z_l}}, \quad (7)$$

$$B_{y,r} = \frac{1 + e^{\alpha z_r} \cos \alpha y}{1 + 2e^{\alpha z_r} \cos \alpha y + e^{2\alpha z_r}}, \quad (8)$$

$$B_{z,r} = \frac{-e^{\alpha z_r} \sin \alpha y}{1 + 2e^{\alpha z_r} \cos \alpha y + e^{2\alpha z_r}}, \quad (9)$$

where $z_l = z + D + L/2$, $z_r = z - D - L/2$, and L is the length of the magnet. Then (assuming an arbitrary B_0) the dipole field is modelled as

$$B_y = B_0(B_{y,l} + B_{y,r} - 1), \quad (10)$$

$$B_z = B_0(B_{z,l} + B_{z,r}). \quad (11)$$

Since the rectilinear cooling dipoles are short, fringe-field-dominated magnets there may be configurations in which the Enge function fringes do not fully converge to 1 in the center (body) of the magnet, i.e.,

$$B_{y,l} + B_{y,r} - 1 < 1 \quad (12)$$

Hence, to ensure that the field at the center of the magnet is equal to B_0 a normalisation factor is computed as

$$\zeta = \frac{1}{(B_{y,l} + B_{y,r} - 1) \Big|_{z=0}} \quad (13)$$

and it is applied to equations 10 and 11. A sample dipole field is shown in Fig. 2.

2.2 Solenoid

Two models have been implemented to estimate the field from a solenoid coil. First, the solenoid is modelled as a single current-carrying sheet. For a more realistic 3D implementation, multiple sheets may be layered upon each other with increasing radii to model a cylindrical block.

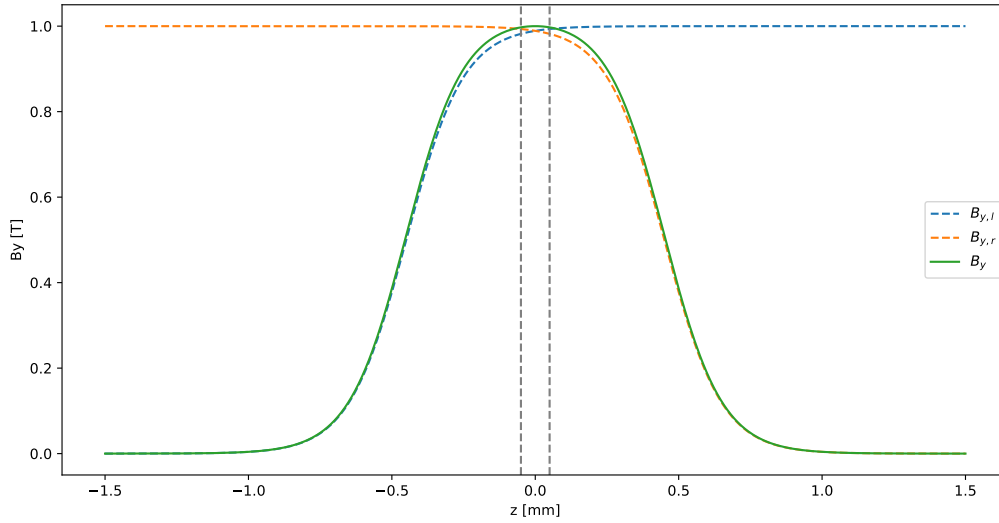


Figure 2: Example B_y dipole field on axis ($x = 0, y = 0$) using model parameters $B_0 = 1$ T, $L = 0.1$ m, $D = 0.4$ m, $a_1 = 4$.

2.2.1 Solenoid Sheet

A solenoid sheet is parameterised by its length $2b$ and radius a , a total current I , and turns per unit length n . The analytic cylindrical magnetic field components follow the treatment outlined by Derby et al. in [10] and have been included below. The coordinates are transformed into cylindrical coordinates as

$$z, \rho, \phi = z, \sqrt{x^2 + y^2}, \arctan\left(\frac{y}{x}\right). \quad (14)$$

Under these coordinates, the radial B_ρ and longitudinal B_z fields are given by

$$B_\rho = B_0 [\alpha_+ C(k_+, 1, 1, -1) - \alpha_- C(k_-, 1, 1, -1)], \quad (15)$$

$$B_z = \frac{B_0 a}{a + \rho} [\beta_+ C(k_+, \gamma^2, 1, \gamma) - \beta_- C(k_-, \gamma^2, 1, \gamma)] \quad (16)$$

where

$$B_0 = \frac{\mu_0 n I}{\pi}, \quad (17)$$

$$z_\pm = z \pm b, \quad (18)$$

$$\alpha_\pm = \frac{a}{\sqrt{z_\pm^2 + (\rho + a)^2}}, \quad (19)$$

$$\beta_\pm = \frac{z_\pm}{\sqrt{z_\pm^2 + (\rho + a)^2}}, \quad (20)$$

$$\gamma = \frac{a - \rho}{a + \rho}, \quad (21)$$

$$k_{\pm} = \sqrt{\frac{z_{\pm}^2 + (\rho - a)^2}{z_{\pm}^2 + (\rho + a)^2}}. \quad (22)$$

$C(\dots)$ stands for the Complete elliptic Integral (C.E.L) and is given by

$$C(k_c, p, c, s) = \int_0^{\pi/2} \frac{c \cos^2 \varphi + s \sin^2 \varphi}{(\cos^2 \varphi + p \sin^2 \varphi) \sqrt{\cos^2 \varphi + k_c^2 \sin^2 \varphi}} d\varphi. \quad (23)$$

The final field is converted back into Cartesian coordinates,

$$B_{x,y,z} = \{B_{\rho}, 0, B_z\}, \quad (24)$$

then rotated about the z axis by angle ϕ .

2.2.2 Solenoid Block

We introduce extra parameters r_{min} , the inner radius of the block, r_{max} , the outer radius of the block, n_s , the number of sheets, and current density J . The i^{th} sheet has radius r_i and current I , where

$$r_i = r_{min} + i(r_{max} - r_{min}) \quad (25)$$

$$I = \frac{J(r_{max} - r_{min})L}{n_s} \quad (26)$$

These parameters are used to initialise solenoid sheets, and generate the magnetic fields using the treatment outlined in the previous section.

2.2.3 Tolerances and bounding boxes

The implementation defines a *spatial tolerance* of

$$10^{-5} \times \min(a, 2b). \quad (27)$$

If the field is requested at a point with radius ρ and longitudinal position z close to a current sheet, such that

$$|\rho - a| < \text{tol.}, \quad |z| < b \quad (28)$$

then no field is returned as the function is unstable at these points.

If the field is queried at a point close to the axis such that

$$|\rho| < \text{tol.}, \quad (29)$$

then a reduced formula of the magnetic field of a solenoid on axis is used, given by:

$$B_z = \frac{\mu_0 n I}{2} \left\{ \frac{z + b}{\sqrt{(z + b)^2 + a^2}} - \frac{z - b}{\sqrt{(z - b)^2 + a^2}} \right\}. \quad (30)$$

We also define the user-supplied *on-axis tolerance* ε . At a given queried point (x, y, z) , if the on axis field $B_z(0, 0, z) < \varepsilon$, $\mathbf{B}(x, y, z) = (0, 0, 0)$ is returned. This helps save compute power by not calculating complicated C.E.L for far away solenoids.

2.3 RF Cavities

The RF cavities are modelled as pillboxes operating in the TM_{010} mode. The electromagnetic field within a cavity is parameterised by the peak electric field E , frequency f , phase ψ , and a global time offset T_0 . The EM field in the cavity is characterized entirely by a longitudinal electric component (E_z) and an azimuthal magnetic component (B_ϕ), given by:

$$E_z(r_n, z, t) = EJ_0(r_n) \cos(2\pi f(t - T_0) + \psi), \quad (31)$$

$$B_\phi(r_n, z, t) = \mu_0 \frac{E}{Z_0} J_1(r_n) \sin(2\pi f(t - T_0) + \psi), \quad (32)$$

Here, J_0 , and J_1 represent bessel functions of the first kind, and r_n is the radial distance normalised to the first zero of J_0 . Z_0 is the impedance of free space and the magnetic field calculation assumes a vacuum.

3 Implementation

3.1 Source Code and Version Control

The underlying code has been written in the C++ language for the BDSIM framework. The code written has been pushed to GitHub, and the changes have also been pulled into the main BDSIM code repository. The code is publicly available and published under GNU General Public License Version 3.

The BDSIM source code can be found at <https://github.com/bdsim-collaboration/bdsim>. The changes documented here have been committed under the SHA: d18134084b3960ba07bea81a7e2772114062f8b3.

3.2 Components

A new BDSIM element, `muoncooler`, has been implemented to enable the simulation of a cooling system. This can be used to define a complete 6D muon cooling lattice. This style of implementation has been chosen such that the fields from each element are summed in superposition to yield a 6-vector electromagnetic field at all points in the channel. This ensures that fringe effects from all magnets are accounted for across the entire lattice.

The `muoncooler` element can easily be placed in a traditional BDSIM lattice. For example, if used to model the Demonstrator, the elements of the transfer line can be modelled with existing BDSIM elements like quadrupoles and dipoles, with the entire muon cooling channel as a single `muoncooler`

element. Upon instantiation, a logical volume with the specified horizontal width and length is generated, providing space for the placement of its components elements.

A cooling channel can include:

- **Solenoids**
- **Dipoles**
- **RF cavities**
- **Absorbers (cylindrical or wedge shaped)**

3.3 Electric and Magnetic Field Models

- The **solenoid field model** can be either a **sheet model** (`solenoidsheet`) or a **block model** (`solenoidblock`).
- For dipoles, two models exist: `dipole` and `dipoleenge`. The `dipole` model represents a simple hard-edge dipole field, while the `dipoleenge` model includes Enge-type fringe fields.
- For RF cavities, a simple RF pillbox (`rfpillbox`) model has been implemented.

3.4 Parameters

The parameters of the `muoncooler` components that have to be specified in the simulation input file are included in Table 1. These parameters can be specified as either:

- A **single value**, applying uniformly across all instances of that component.
- A **list of values**, where each value corresponds to the respective component's position in the cooling channel.

Parameter	Description	Type
nCoils	Number of solenoid coils in the cooling channel	Integer
coilInnerRadius	Inner radii of coils [m]	List[Float]
coilRadialThickness	Radial thicknesses of coils [m]	List[Float]
coilLengthZ	Lengths of coils along Z [m]	List[Float]
coilOffsetZ	Z-positions of coil centers [m]	List[Float]
coilCurrent	Currents in [A] (sheet model) or densities [A/m ²] (block model)	List[Float]
coilMaterial	Materials of coils	List[String]
onAxisTolerance	On-axis tolerance for CEL integral calculation [T]	Float
nDipoles	Number of dipoles	Integer
dipoleAperture	Aperture radii of dipoles [m]	List[Float]
dipoleLengthZ	Lengths of dipoles along Z [m]	List[Float]
dipoleFieldStrength	Peak magnetic field strengths of dipoles [T]	List[Float]
dipoleEngeCoefficient	C1 Enge coefficients of dipoles	List[Float]
dipoleOffsetZ	Z-positions of dipoles [m]	List[Float]
nAbsorbers	Number of absorbers	Integer
absorberType	Types of absorbers (cylinder or wedge)	List[String]
absorberMaterial	Materials of absorbers	List[String]
absorberOffsetZ	Z-positions of absorbers [m]	List[Float]
nRFCavities	Number of RF cavities	Integer
rfOffsetZ	Z-positions of RF cavities [m]	List[Float]
rfTimeOffset	Time offsets for RF cavities [ns]	List[Float]
rfLength	Inner lengths of RF cavities [m]	List[Float]
rfVoltage	Peak E-Field of RF cavities [MV/m]	List[Float]
rfPhase	Phases of RF cavities [rad]	List[Float]
rfFrequency	Frequencies of RF cavities [Hz]	List[Float]
rfWindowMaterial	RF window material	List[String]
magneticFieldModel	Model for solenoid field	String
dipoleFieldModel	Model for dipole field	String
electricFieldModel	Model for RF electric field	String
l	Length of the cooling channel [m]	Float
horizontalWidth	Width of the cooling channel [m]	Float

Table 1: Table of Parameters of the components of the cooling channel.

An example of a cooling channel is provided in the BDSIM GitHub repository. This can be found in `bdsim/examples/components/muoncooler.gmad`, and can be used as a template for further designs.

3.5 Visualisation

BDSIM allows for GEANT4 visualisations of lattices. A 3D rendering of an example cooling channel consisting of 3 cells with 2 absorbers is shown in Fig. 3.

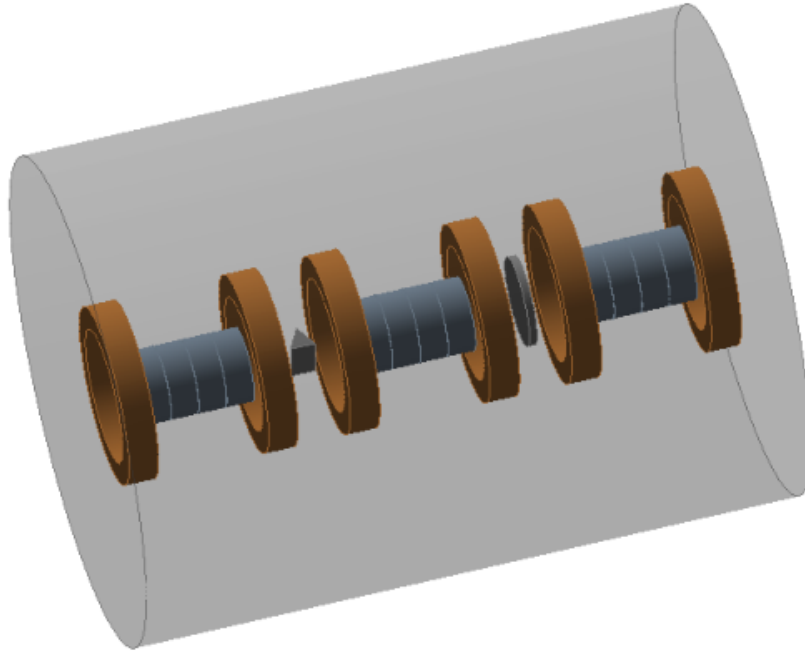


Figure 3: A 3D rendering of a cooling channel simulated using BDSIM.

4 Validations

The following section details the validations carried out on the code and first cooling demonstrations. First, each constituent component was validated separately. Simulations were compared to analytic formulae, and/or other tracking codes such as G4Beamline. Then, simulations of muon beams traversing entire cooling channels were produced, showing 4D and 6D cooling.

4.1 Dipole

First, a comparison of the BDSIM output field map with the Python output of the analytical model described in Section 2.1 was made. A `muoncooler` element with one dipole field with Enge fringes was defined. The dipole parameters fed into the BDSIM input file are shown in Table 2. The B_y and B_z field comparisons are shown in Figures 4 and 5, respectively. Agreement is observed both on and off axis ($y = 10$ cm), as seen in the residual plots which indicate a 10^{-7} T level discrepancy.

Next, a comparison with G4Beamline was performed. The dipole arrangement and parameters of the MuCol Rectilinear A Stage 1 lattice [11; 12] were reproduced in BDSIM. Each cooling cell contains two dipoles with identical field strength and polarity. Due to the close proximity to the adjacent cells and large fringe field regions, the dipole field within a cell is impacted by the neighbouring cells. The

Parameter	Unit	Value
Aperture radius	m	0.2
Magnet length	m	0.1
Field strength	T	1
Enge coefficient	-	5.5

Table 2: Dipole parameters used to model one Enge dipole field in BDSIM.

parameters of the dipoles in the lattice are shown in Table 3.

Parameter	Unit	Value
Aperture radius	m	0.3
Magnet length	m	0.1
Field strength	T	0.03918
Enge coefficient	-	5.5

Table 3: Parameters of the dipoles used in the G4Beamline comparison.

The B_y field generated by the dipole lattice is shown in Fig. 6, on and off axis ($y = 10 \text{ cm}$). The field is shown over the extent of one cooling cell, with the boundaries of two dipole magnets indicated by the vertical gray lines. The residuals between the fields produced by the two codes are also shown. Good agreement is observed - the residuals indicate discrepancies of $\mathcal{O}(10^{-4} \text{ T})$ on axis and $\mathcal{O}(10^{-5} \text{ T})$ at $y = 10 \text{ cm}$. The discrepancies are explained by the different implementation of the field model - in G4Beamline, the field is constant over the extent of the magnet with the left and right fringe fields appended either side of this central constant field. As the Enge-type fringes do not fully converge to the value of the field in the body of the magnet, this leads to discontinuities at the magnet boundaries, which become apparent as jumps in the residuals and give rise to the observed discrepancy. The further off axis, the quicker the fringe fields converge, leading to reduced discontinuities and hence differences between the two codes.

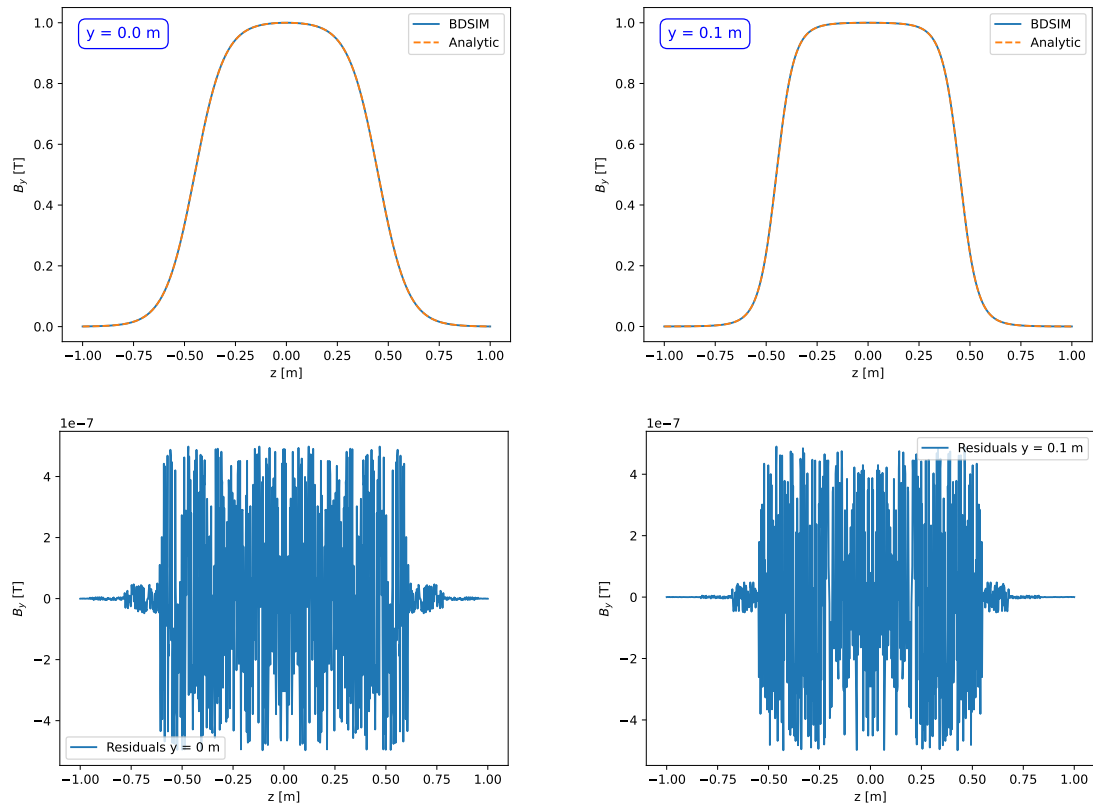


Figure 4: (top) B_y field profile. The blue line represents the BDSIM output; the orange dashed line represents the analytic formula output. (bottom) Residuals between the two field-generating methods. Both the fields and residuals are shown for (left) $y = 0$ m and (right) $y = 0.1$ m.

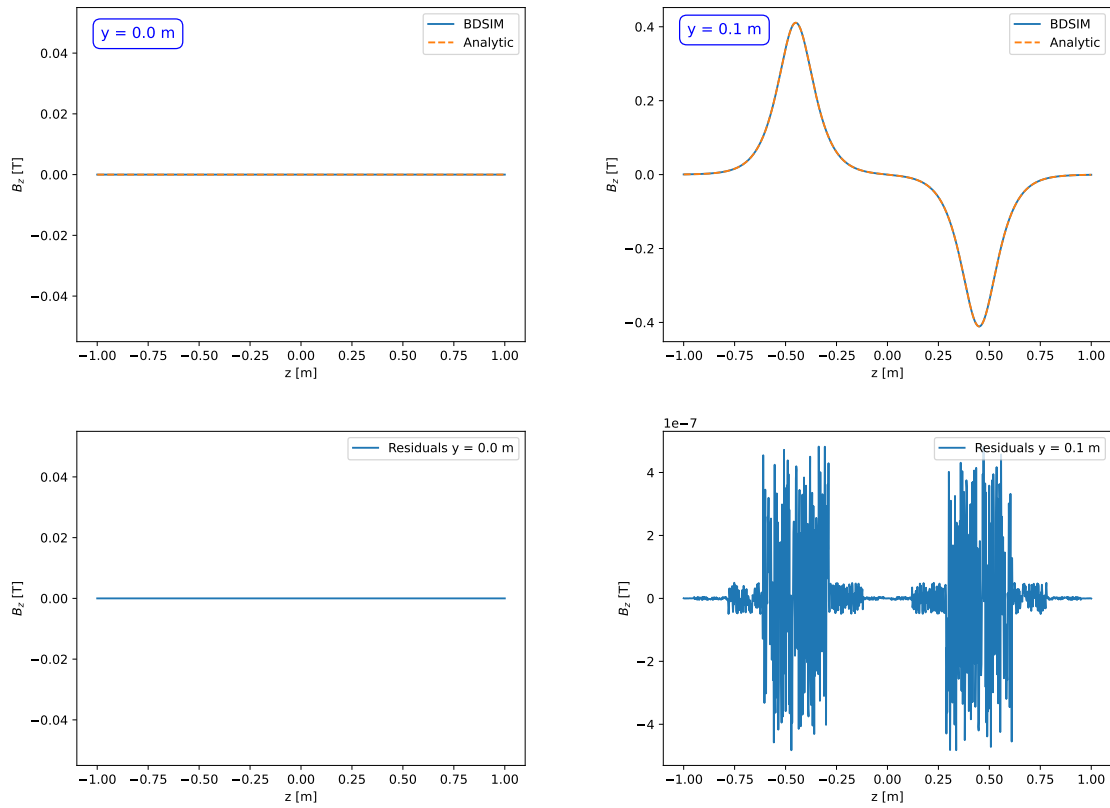


Figure 5: (top) B_z field profile. The blue line represents the BDSIM output; the orange dashed line represents the analytic formula output. (bottom) Residuals between the two field-generating methods. Both the fields and residuals are shown for (left) $y = 0$ m and (right) $y = 0.1$ m.

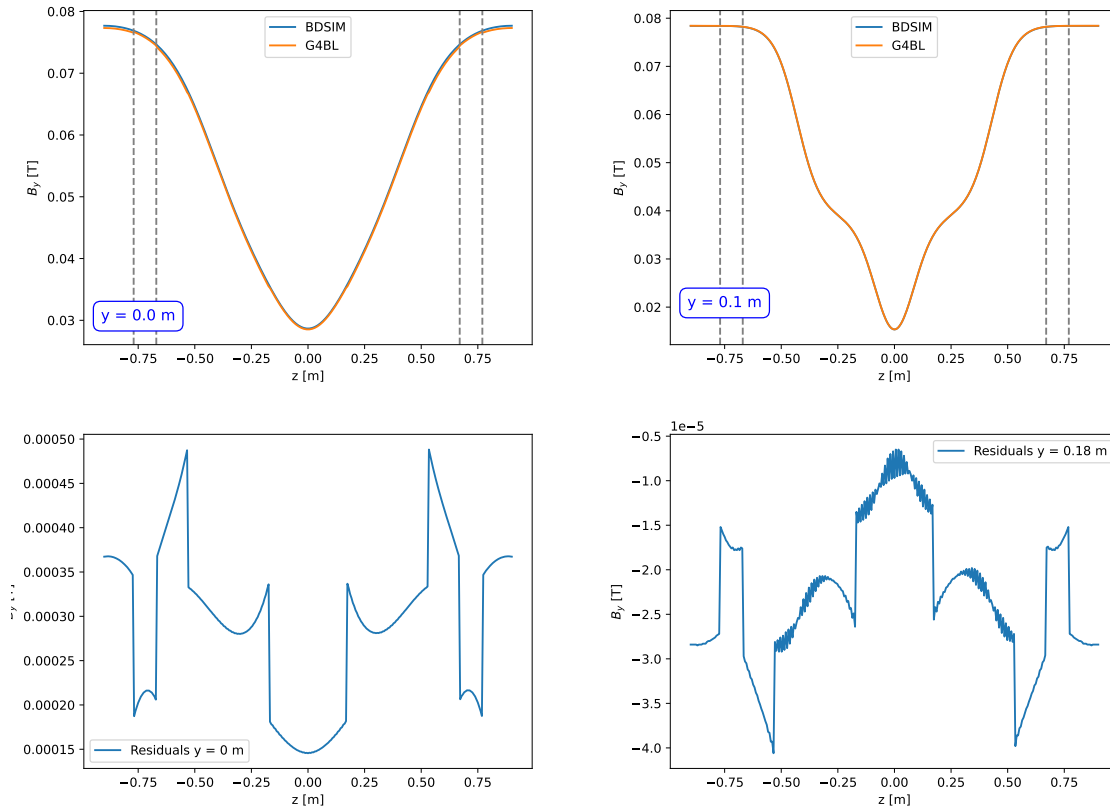


Figure 6: (top) B_y field profile of the Rectilinear A Stage 1 cooling cell. The blue line represents the BDSIM output; the orange line represents the G4Beamline output. (bottom) Residuals between the output of the two codes. Both the fields and residuals are shown for (left) $y = 0$ m and (right) $y = 0.1$ m.

4.2 Solenoid

Parameter	Unit	Value
Inner Radius	m	0.25
Thickness	m	0.1693
Length	m	0.14
Current Density	Am ⁻²	500
Material	-	G4_Cu
Tolerance	-	0
Sheets	-	20

Table 4: Solenoid parameters.

The field map for a solenoid block was generated and the following longitudinal (B_z) and transverse (B_x) fields were generated.

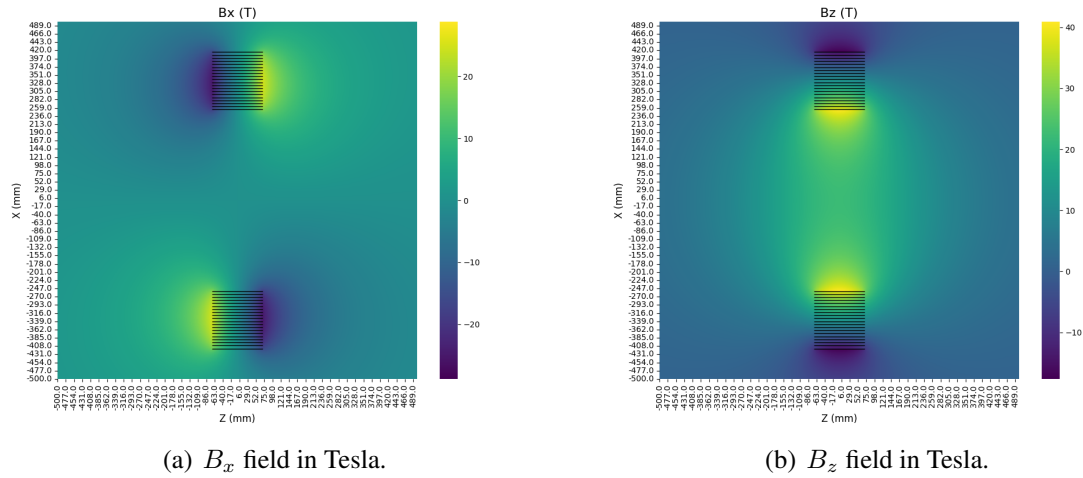


Figure 7: Transverse (B_x) and longitudinal (B_z) magnetic fields of the tracked solenoids. The horizontal lines on the plot indicate the position of the sheets.

The field maps were compared against G4Beamline field maps for a solenoid with the same parameters. Fields are shown in Fig. 7 and residuals are shown in Fig. 8 and 9, showing agreement at 10^{-3} level.

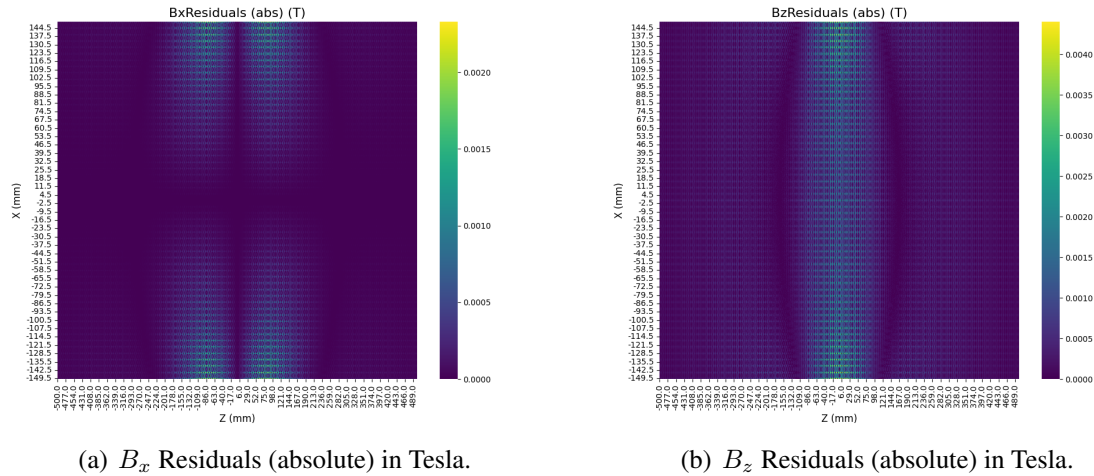


Figure 8: Absolute residuals of the B_x and B_z field components, illustrating deviations from the expected field values.

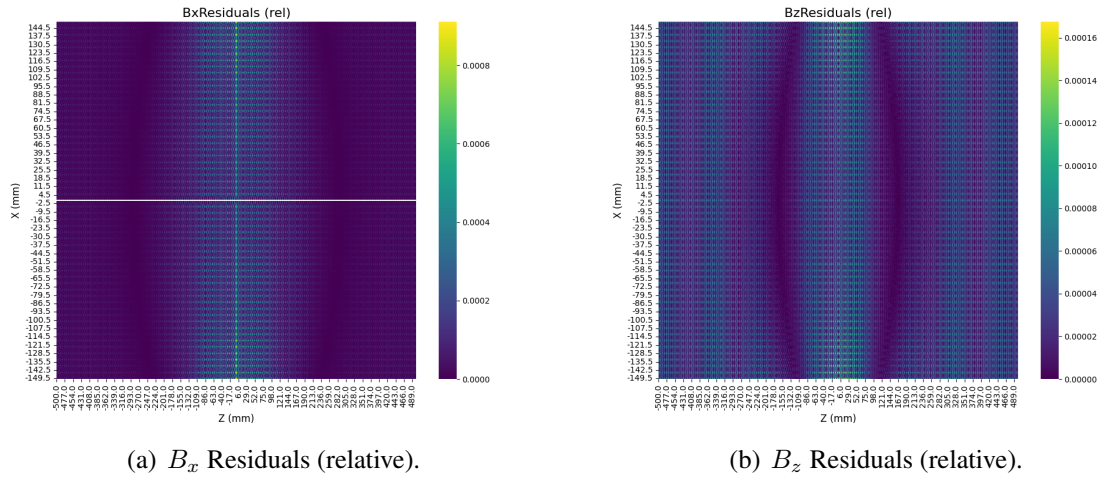


Figure 9: Relative residuals of the B_x and B_z field components, showing fractional deviations from expected values.

A set of particles were tracked through the field of single solenoid and the output was compared against an identical G4Beamline study. 200 MeV/c muons were initialised along a grid on the x -axis, between 0 mm and 200 mm in separations of 10 mm. Tracking started from 0.5 m upstream of the solenoid. Fig. 10 compares BDSIM and G4Beamline positions 0.5 m downstream of the solenoid, showing very good agreement.

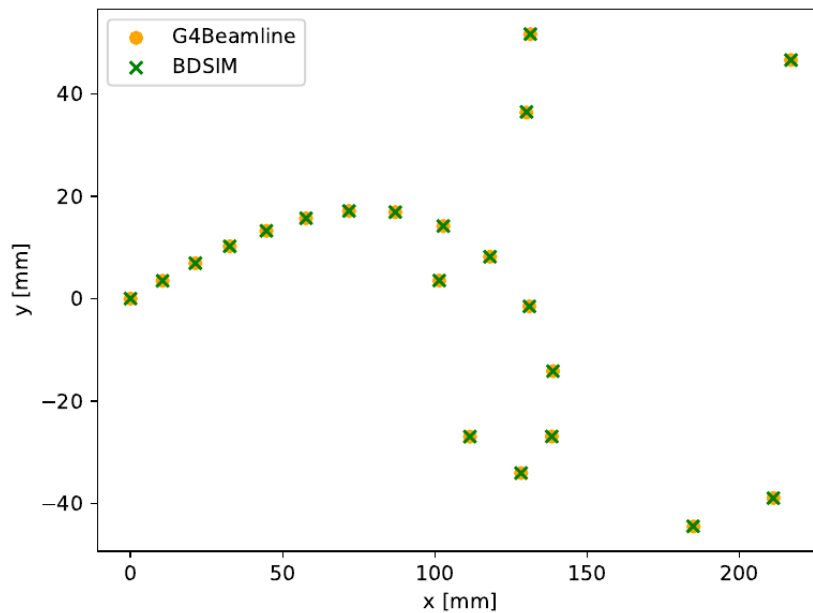


Figure 10: Comparison of particle positions after tracking through a single solenoid using BDSIM and G4Beamline.

4.3 RF Cavities

A single RF cavity with the parameters shown in Table 5 was modelled. The electric and magnetic fields were queried at $t = 0$ and after one quarter of an RF period ($t = 1/2816 \mu\text{s}$) at the longitudinal centre of the cavity.

Parameter	Unit	Value
Length	m	0.18856
Peak E Field	MV/m	30
Phase	°	0
Frequency	MHz	704

Table 5: RF Cavity Parameters.

The resulting fields are shown in Fig. 11. The simulated fields were then compared to the corresponding analytic calculations to assess their accuracy and the residuals are shown in Fig. 12. The results demonstrate good agreement between the simulation and the theoretical predictions.

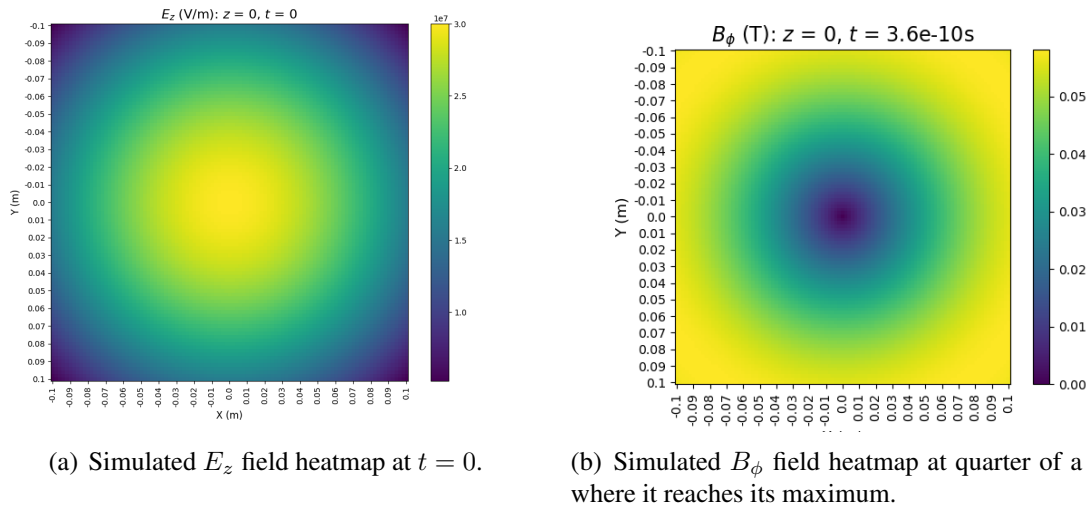


Figure 11: Simulated (left) E_z and (right) B_ϕ field heatmaps at different time points within the RF cycle.

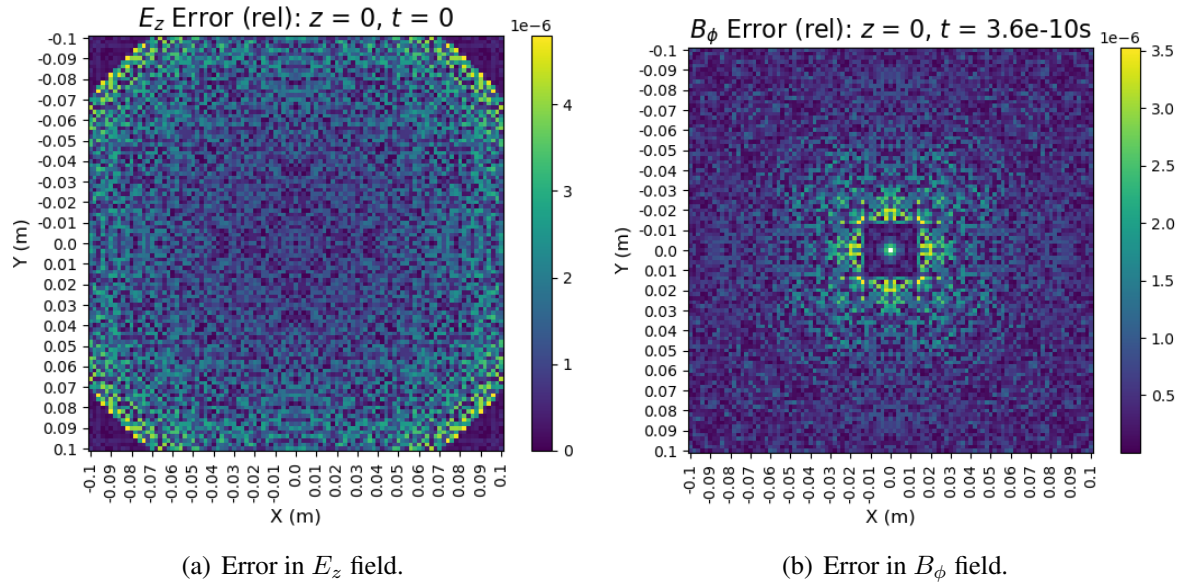


Figure 12: Errors in simulated (left) E_z and (right) B_ϕ fields against analytical calculations.

The error plots confirm that the simulated fields show agreement with the analytic expectations at a 10^{-6} level.

4.4 Absorbers

The absorbers were validated by comparison against other simulation codes. Simulations using lithium hydride (LiH) or Liquid Hydrogen (LH) absorbers were carried out to compare the energy loss and scattering models. The absorbers were cylindrical, with thicknesses shown in Table 6.

Material	Unit	Thickness
Lithium Hydride	mm	65
Liquid Hydrogen	mm	350

Table 6: Thickness of the two absorbers studied.

The scattering and momentum distribution plots shown here (Figs. 13 and 14) have been adapted from [13]. In all cases, BDSIM shows good agreement with G4Beamline and ICOOL. RF-Track, which is also under development, exhibits a discrepancy in the momentum distribution at the exit of the absorber, as it currently uses a simplistic Gaussian energy loss model.

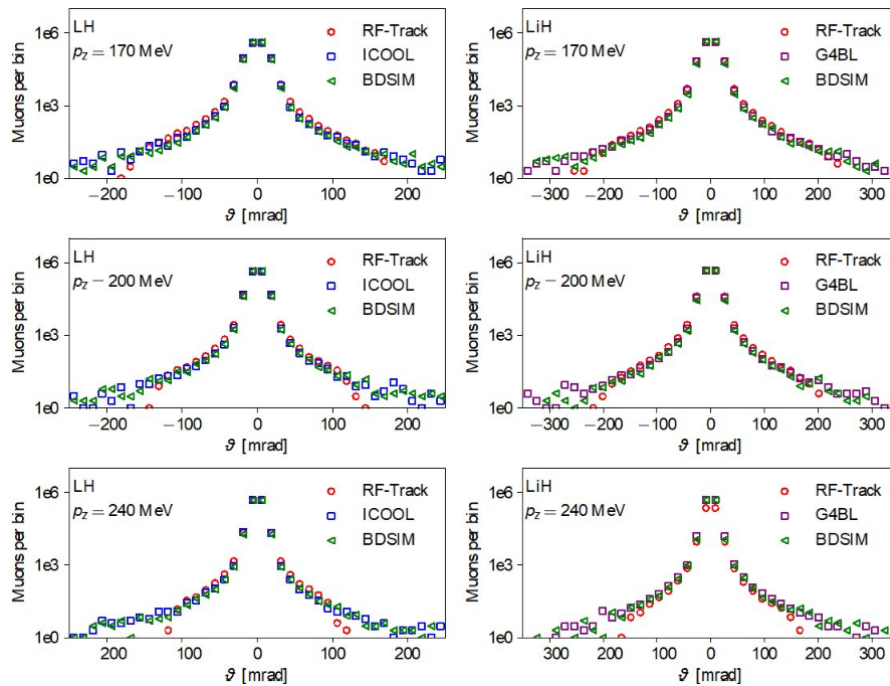


Figure 13: Distribution of projected angles following simulated scattering in (left) LH and (right) LiH absorbers, at three different beam momenta: (top) 170 MeV/c, (center) 200 MeV/c and (bottom) 240 MeV/c.

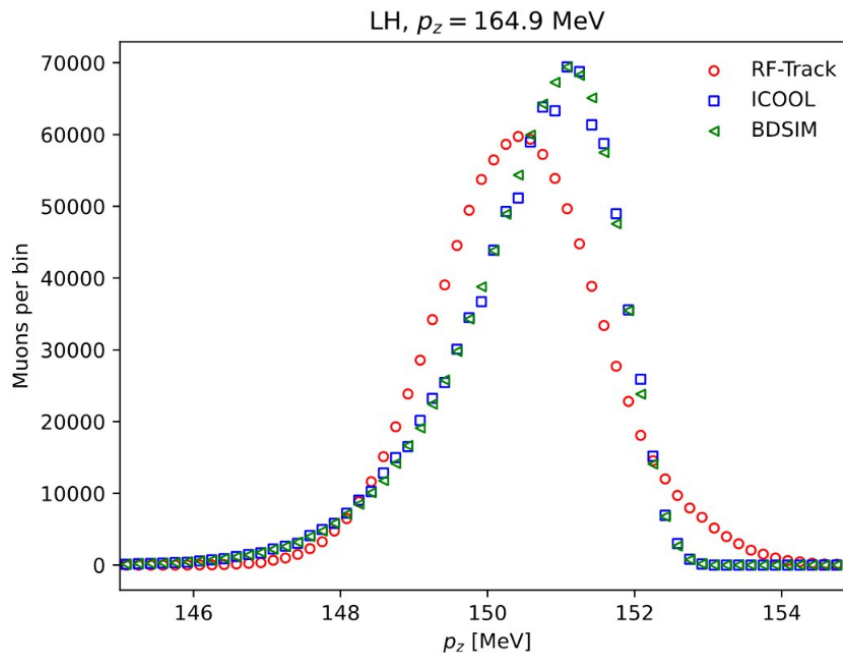


Figure 14: Final muon momentum distribution of a monoenergetic incident beam passing through a LH absorber.

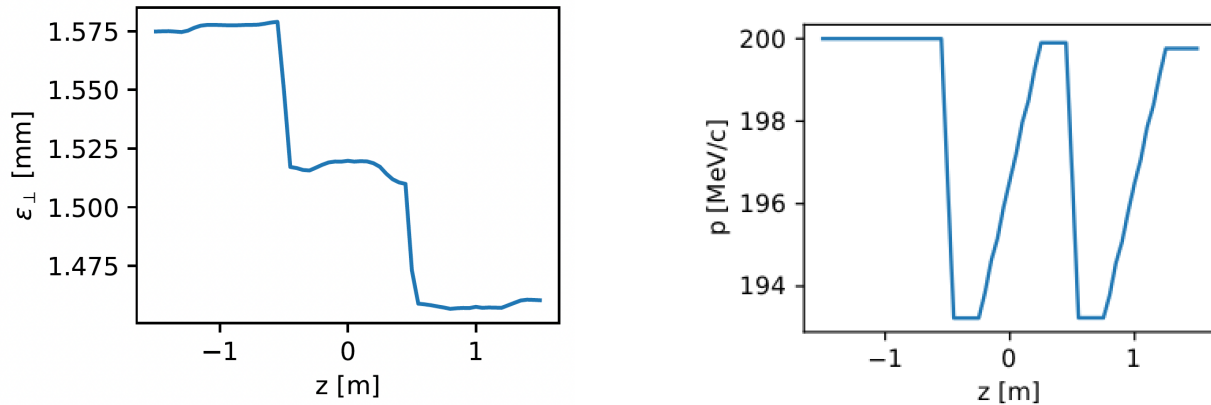
4.5 Full Lattice

Along with validations of the individual components, demonstrations of 4D and 6D cooling lattices were carried out. First, a simple 4D cooling lattice was set up using the solenoid lattice parameters presented in [14]. Then a 80 m-long 6D cooling lattice based on the cell design presented in [8] was simulated.

4.5.1 4D Cooling

The short 4D cooling lattice studied here is composed of three cooling cells, with two cylindrical lithium hydride absorbers placed at the cell boundaries. The lattice does not include dipoles or wedge absorbers, and since no dispersion is induced, the beam is cooled only in the transverse plane. This represents both an important milestone toward the full simulation of a rectilinear cooling channel and a proof of concept that BDSIM can be used to simulate final cooling section of the muon collider cooling system. More details on the lattice setup can be found in [15].

The main results of the study, presented at IPAC24 [15], are shown in Fig. 15. The transverse emittance of the beam is reduced in the two absorbers located at $z = -0.5$ m and $z = 0.5$ m.



(a) Reduction of the transverse beam emittance as it propagates through the cooling channel.

(b) Mean momentum evolution of the beam as it passes through the absorbers, losing momentum before regaining it in the RF cavities.

Figure 15: Transverse emittance and momentum evolution of the beam in the cooling channel.

4.5.2 Rectilinear (6D) Cooling

Following the implementation of dipole field models in the BDSIM `muoncooler` element, a rectilinear cooling lattice was simulated. The lattice is based on the Muon Cooling Demonstrator cooling cell presented in [8] and shown in Fig. 1. The detailed description of the cooling cell can be found in Table 2 of that document.

First, a solenoid lattice was set up using the solenoid block model. The resulting on-axis B_z field profile over the extent of one cooling cell is shown in Fig. 16. In this figure, the BDSIM output is compared with an ideal solenoid field based on the sum of two harmonic components, defined as

$$B_z(z) = b_1 \sin\left(\frac{2\pi z}{L}\right) + b_2 \sin\left(\frac{4\pi z}{L}\right), \quad (33)$$

where L is the length of the cooling cell, and b_1 and b_2 are the amplitudes of the respective harmonics. For this cooling cell design iteration, the parameters were set to $b_1 = 8.75$ T, $b_2 = 1.25$ T and $L = 0.8$ m. BDSIM, because it uses a more realistic field model, was not expected to agree perfectly with the ideal field model. The two models showed satisfactory agreement.

The optical beta function along the cooling cell for a 200 MeV/c beam is shown in Fig. 17. It presents minima at the extremities of the cooling cell, where the absorbers are located, indicating a tight focus.

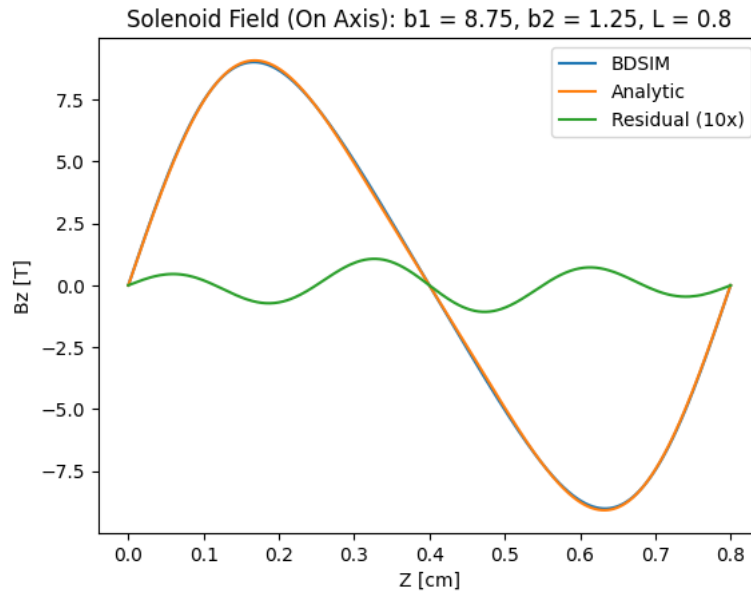


Figure 16: Cooling cell on-axis B_z , for (blue) BDSIM and (orange) ideal field. The green line shows the residuals between the two fields multiplied tenfold.

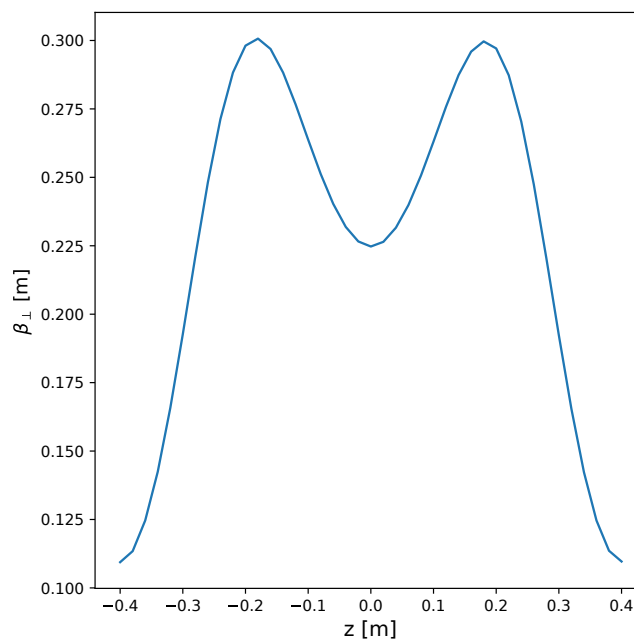


Figure 17: Optical beta function over the extent of the cooling cell for a 200 MeV/c beam.

Dipoles were added to create dispersion. The dipole field was modelled as a vertical hard-edge field. Further studies and comparisons with G4Beamline will make use of the more realistic Enge fringe fields model available in BDSIM. The x and y closed-orbit trajectories over the extent of two cooling cells for three different momenta are shown in Fig. 18. The two-cell periodicity of the closed orbits is the result of flipping the dipole polarities every other cell. Significant dispersion is observed at the locations of the absorbers, particularly in the x plane, as intended.

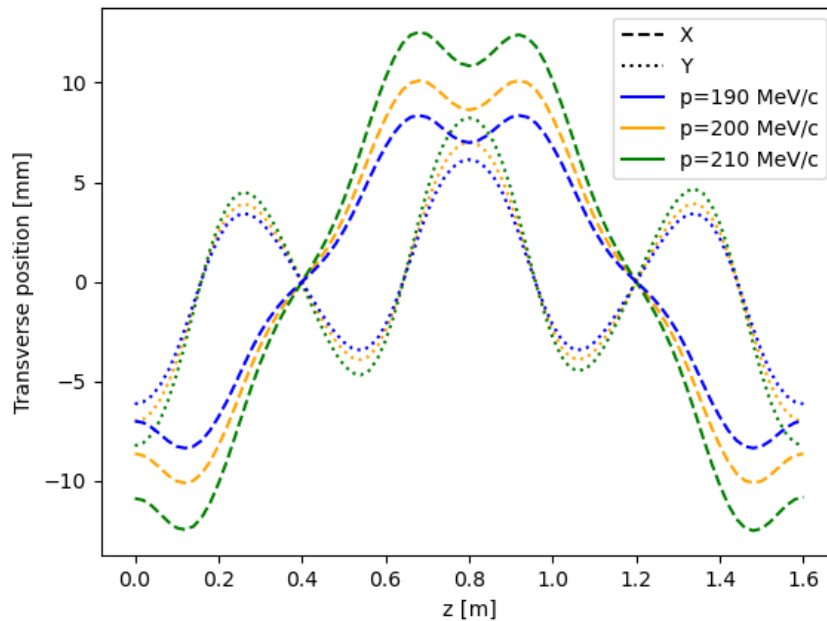


Figure 18: x and y closed orbit trajectories at three different momenta.

Finally, the 704 MHz RF cavities and lithium hydride wedge absorbers (20 mm thickness on axis) were added to the lattice, and a full beam was tracked through a ~ 80 m-long cooling channel. The initial beam was a multivariate Gaussian, with ~ 2.5 mm transverse emittance and ~ 1.8 eV s longitudinal emittance. The cooling performance of the lattice is shown in Fig. 19.

Transverse and longitudinal cooling is observed. A mismatch occurs in the longitudinal phase space leading to an initial emittance growth, causing losses in the beam tails. Additionally, the mismatch leads to beam momentum oscillations which translate into an oscillating behaviour of the longitudinal emittance. These effects could be mitigated by preparing an appropriately matched beam. Furthermore, the development of a more robust analysis technique to remove the tail events that bias the emittance calculation will help better capture the cooling in the core of the beam.

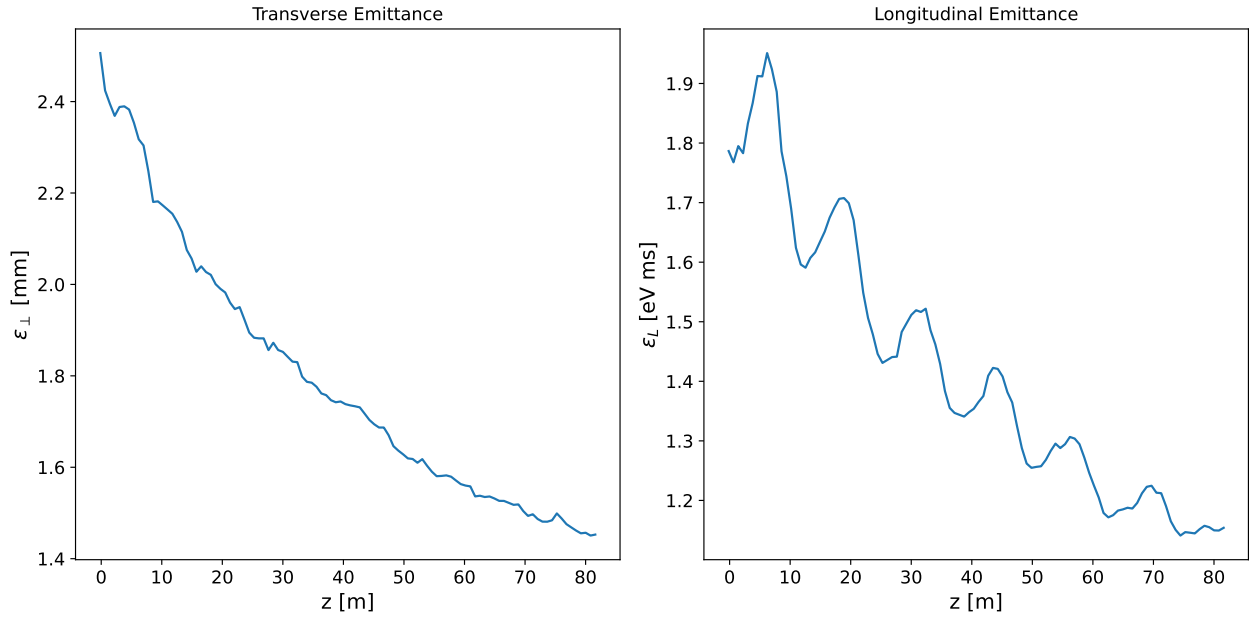


Figure 19: The evolutions of the (left) transverse and (right) longitudinal emittances across a ~ 80 m lattice.

5 Conclusion and Future Work

A `muoncooler` beamline element has been implemented in BDSIM. The individual components were validated against analytic models or suitable codes such as G4Beamline. Finally, demonstrations of 4D and 6D cooling were produced. This development renders BDSIM as a code suitable for simulating the full ionisation cooling complex of the muon collider.

Next steps in the development of this code and its adoption as a muon cooling simulation tool consist in 6D cooling benchmarking against G4Beamline and potentially RF-Track. Additionally, further optimisations aimed at making the code more efficient and realistic are planned. For example, the field map could be stored on a grid in memory, and interpolation could be used to query the field during tracking.

References

- [1] Bogomilov M, Tsenov R, Vankova-Kirilova G, Song YP, Tang JY, Li ZH, et al. Transverse emittance reduction in muon beams by ionization cooling. *Nature Physics*. 2024 10;20(10):1558-63.
- [2] Accettura C, others. MuCol Milestone Report No. 5: Preliminary Parameters. 2024 2.
- [3] Roberts TJ, Kaplan DM. G4beamline simulation program for matter-dominated beamlines. In: 2007 IEEE Particle Accelerator Conference (PAC). IEEE; 2007. p. 3468-70.
- [4] Latina A. RF-Track Reference Manual. Zenodo; 2020. Available from: <https://doi.org/10.5281/zenodo.3887085>.
- [5] Nevay LJ, Boogert ST, Snuverink J, Abramov A, Deacon LC, Garcia-Morales H, et al. BDSIM: An accelerator tracking code with particle-matter interactions. *Computer Physics Communications*. 2020 7;252:107200.
- [6] Agostinelli S, Allison J, Amako K, Apostolakis J, Araujo H, Arce P, et al. Geant4—a simulation toolkit. *Nuclear Instruments and Methods in Physics Research Section A: Accelerators, Spectrometers, Detectors and Associated Equipment*. 2003 7;506(3):250-303.
- [7] Nevay L. Development of BDSIM for muon simulations; 2021. Available from: <https://indico.stfc.ac.uk/event/362/contributions/2280/>.
- [8] Losito R, Rossi L, Barbagallo C, Berg JS, Bottura L, Burt G, et al.. Presentation of cooling cell conceptual design. Zenodo; 2024. Available from: <https://doi.org/10.5281/zenodo.11402737>.
- [9] Muratori Bones Jolski A. Analytical expressions for fringe fields in multipole magnets. *Physical Review Special Topics - Accelerators and Beams*. 2015 6;18(6):064001.
- [10] Derby N, Olbert S. Cylindrical magnets and ideal solenoids. *American Journal of Physics*. 2010 3;78(3):229-35.
- [11] Zhu R. MuonCollider-WG4 - Lattice ; 2024. Available from: https://github.com/MuonCollider-WG4/rectilinear/tree/main/2024-8-12_lattice_files/pre_merge/stage1.
- [12] Zhu R, Rogers C, Yang J, Zhao H, Guo C, Li J. Performance and tolerance study of the rectilinear cooling channel for a }muon collider. *arXiv (Cornell University)*. 2024 2.
- [13] Stechauner B. Simulation software for ionisation cooling; 2024. Available from: <https://indico.fnal.gov/event/64984/contributions/299934/>.
- [14] Rogers C. A Demonstrator for Muon Ionisation Cooling. In: NuFACT 2022. Basel Switzerland: MDPI; 2023. p. 37.
- [15] Kamath R, Rogers C, Jurj P. Simulating a 6D cooling channel in BDSIM. *JACoW*. 2024;IPAC2024:TUPC20.